Recent Results from CLEO I and A Glance at CLEO II Data

Yuichi Kubota
University of Minnesota, Minneapolis, MN 55455

Abstract

We present highlights of results based on 428 pb^{-1} of e^+e^- annihilation data taken with the CLEO I detector at CESR (Cornell Electron Storage Ring). Measuring the branching fractions for $B^- \to D^0 l^- \bar{\nu}$ and $\bar{B}^0 \to D^+ l^- \bar{\nu}$ we estimate that $|V_{bc}| \sim 0.040$. The ratio of semileptonic widths for final states with vector and pseudo-scalar D mesons are determined to be 2.6 ± 1.1, and the ratio of B^- and $\bar{B}^0$ lifetimes, $\tau(B^-)/\tau(\bar{B}^0) = 0.89 \pm 0.19 \pm 0.13$. We have observed the decay $D_S^+ \to \phi l^+ \nu$, which leads to a determination of absolute D_S^+ decay branching fractions. The asymmetry we have observed in the decay $\Lambda_C^+ \to \Lambda \pi^+$ demonstrates a violation of parity conservation in the weak decay of a charmed particle. The CLEO II detector started operation in the fall of 1989. We report on the performance of its CsI calorimeter.

I. Introduction

The e^+e^- annihilation data used in the analyses we report here were collected with the CLEO I detector in 1987 at Cornell Electron Storage Ring (CESR). 212 pb^{-1} of the data were taken on the $\Upsilon(4S)$ resonance, 102 pb^{-1} of the data, at an energy below the $\Upsilon(4S)$, and 116 pb^{-1} of the data, on the $\Upsilon(5S)$ resonance. In B physics analyses, the former two sets of data are used. The second set is used to estimate the contribution of continuum e^+e^- annihilations in the first. In the other analyses, all three sets are used.

The CLEO detector[1] went through a major upgrade in its tracking system. The main drift chamber consists of 51 layers of wires, 11 of which are stereo, and cathode pads on the inner and outer walls. It measures the specific ionization of particles to a 6.5% accuracy.[2] Inside the main chamber is a 10-layer vertex chamber with cathode pads. The innermost chamber provides additional three layers of tracking with straw tubes.[3] The momentum resolution using the whole system is $(\delta p/p)^2 = (0.23\%p)^2 + (0.7\%)^2$, where p is in GeV/c.

One of the most recent results in B physics is the measurements of the branching fractions for the decay $B^- \to D^0 l^- \bar{\nu}$ and $\bar{B}^0 \to D^+ l^- \bar{\nu}$. We discuss these measurements as well as their implications in Chapter II. We have observed the decay $D_S^+ \to \phi l^+ \nu$, which allows us to calculate the branching fractions of D_S^+ decays, as reported in Chapter III. In Chapter IV, we describe the observation of a non-zero helicity polarization of the Λ in the decay $\Lambda_c^+ \to \Lambda \pi^+$, which demonstrates a violation of parity conservation in the weak decay of a charmed particle. Finally, in Chapter V, we demonstrate the high performance of the CsI-crystal calorimeter.

II. $B \to D l^- \bar{\nu}$[4]

QCD effects in semileptonic B decays can be summarized in terms of form factors, and are easier to understand than hadronic decays. We calculate the Kobayashi-Maskawa matrix element V_{cb} in a way similar to the way V_{ud} and V_{us} were measured using pseudo-scalar meson decays.[5] The differential decay rates as functions of momentum transfer, q^2, lepton momentum, p_l, and the polarization of the charmed meson (if it is a D^*) would provide constraints on the form factors which have been estimated by various models.[6,7,8]

We present the first measurements of the exclusive branching fractions $B(B^- \to D^0 l^- \bar{\nu})$ and $B(B^- \to D^{*0} l^- \bar{\nu})$ and a new measurement of $B(\bar{B}^0 \to D^+ l^- \bar{\nu})$. Using the average of $B(B^- \to D^0 l^- \bar{\nu})$ and $B(\bar{B}^0 \to D^+ l^- \bar{\nu})$ we calculate $|V_{bc}|$. Then combining $B(\bar{B}^0 \to D^{*+} l^- \bar{\nu})$[9] with the current results, we derive the lifetime ratio of the B^- and $\bar{B}^0$, τ^-/τ^0, and the ratio of vector meson (D^*) and pseudo-scalar meson (D) productions in the semileptonic B decay.

We search for the decays $D^0 \to K^- \pi^+$ and $D^+ \to K^- \pi^+ \pi^+$ in events with at least one lepton candidate. Figure 1 shows the $K^- \pi^+$ and $K^- \pi^+ \pi^+$ invariant mass distributions in $\Upsilon(4S)$ and continuum samples. Existence of the D^0 and D^+ in these events is evident. Many processes contribute to these signals. They are:

(a) $B \to D l \bar{\nu}$ decays.
(b) $B \to D^* l \bar{\nu}$ decays, where we ignore π's or γ's from D^* decays.
(c) $B \to D^{**} l \bar{\nu}$ decays or $B \to D^{(*)} X l \bar{\nu}$ decays, where X=nπ's. Since we cannot distinguish these two, we consider them together.
(d) $\Upsilon(4S) \to B^0 \bar{B}^0$, $\bar{B}^0 \to DX$ and $B^0 \to$mixing$\to \bar{B}^0 \to l^- X$; or $\Upsilon(4S) \to B\bar{B}$, $\bar{B} \to DX$ and $B \to \bar{D} X$ followed by $\bar{D} \to l^- X$. The latter contributes many fewer events.
(e) lepton candidates are misidentified hadrons (fake leptons).
(f) continuum contribution.

The continuum contribution (f) is reduced using a difference in event shapes between $B\bar{B}$ and continuum events. We require that the ratio of Fox-Wolfram moments R_2 be less than 0.4. With this cut only 5% of spherical $B\bar{B}$ events are lost while 55% of the continuum events are rejected. The remaining continuum contribution is removed statistically by subtracting properly scaled continuum data from the $\Upsilon(4S)$ data. Fake lepton contribution (e) is subtracted using hadron misidentification probability and the number of events which have D and potential

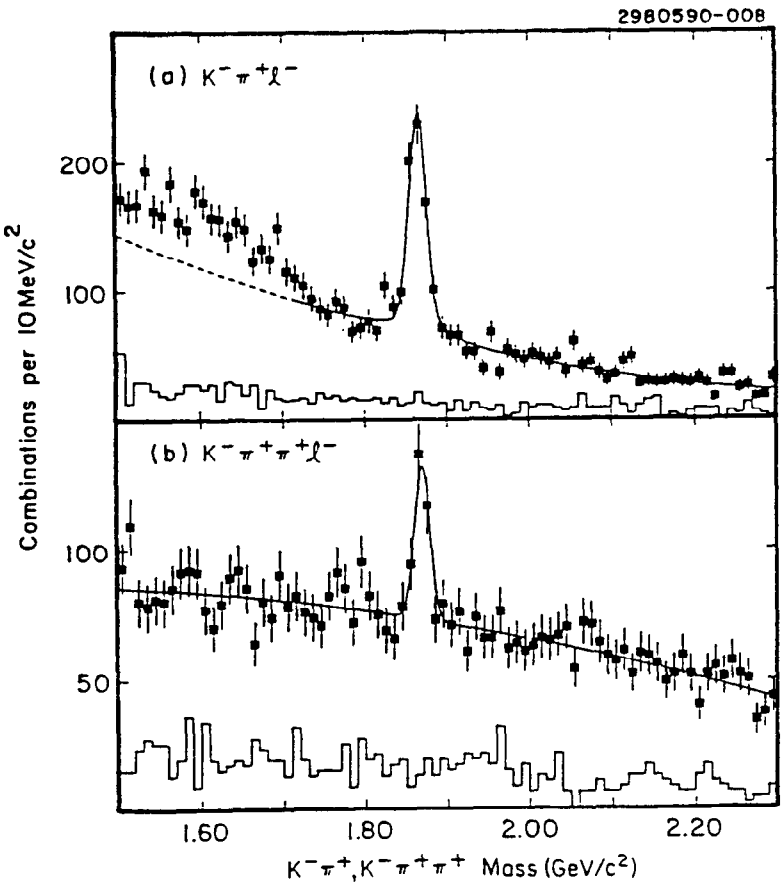

Figure 1. Invariant mass distributions for D candidates in events containing identified leptons. The histograms show scaled continuum data. The solid lines are the fits to the spectra.

l^- candidates (tracks which satisfy the same fiducial volume requirement that lepton candidates are subject to). The hadron misidentification probability is calculated using a lepton poor $Y(1S)$ decay sample, as well as a sample of π's and protons from K^0_S and Λ decays which are identified using their separate secondary vertices.

Since $B^0\bar{B}^0$mixing is the major source of (d), knowing the mixing rate[10] we can calculate its relative contributions to Dl^- and Dl^+ final states [the latter state results from process (d) if B does not mix]. By counting the number of Dl^+ candidates [which are mostly from process (d)], we can, therefore, estimate[11] the number of Dl^- due to this process (d). Before we subtract this background, we attempt to reduce it using its difference in kinematics from signal processes we are interested in, namely, processes (a-c). Since while D and l^- tend to be in the opposite hemisphere in the processes (a-c), there is no direction correlation between the two particles in the background process (d). Therefore, we require that the angle between the D and l^-, θ_{Dl^-} satisfy $cos\theta_{Dl^-}<0$. We remove the remaining contribution from process (d) in our sample by subtracting the properly scaled Dl^+ sample.

We use distributions of the missing mass squared (MM) of the system recoiling against Dl^- (the mass of X for the decay $B\rightarrow Dl^-X$), in order to distinguish various contributions. As seen in Figure 2, the distributions of those candidates from (a-c) will center around MM=0, whereas the one from (d) extends to large negative values. We obtain the Dl^- yield in a given MM interval by plotting $K^-\pi^+(\pi^+)$ invariant mass distributions for combinations whose MM falls in that interval. Then we fit them with a Gaussian representing the D signal and a polynomial background. Figure 3 shows MM distributions obtained in this way for $D^+l^-$and D^0l^- candidates. When we subtract the

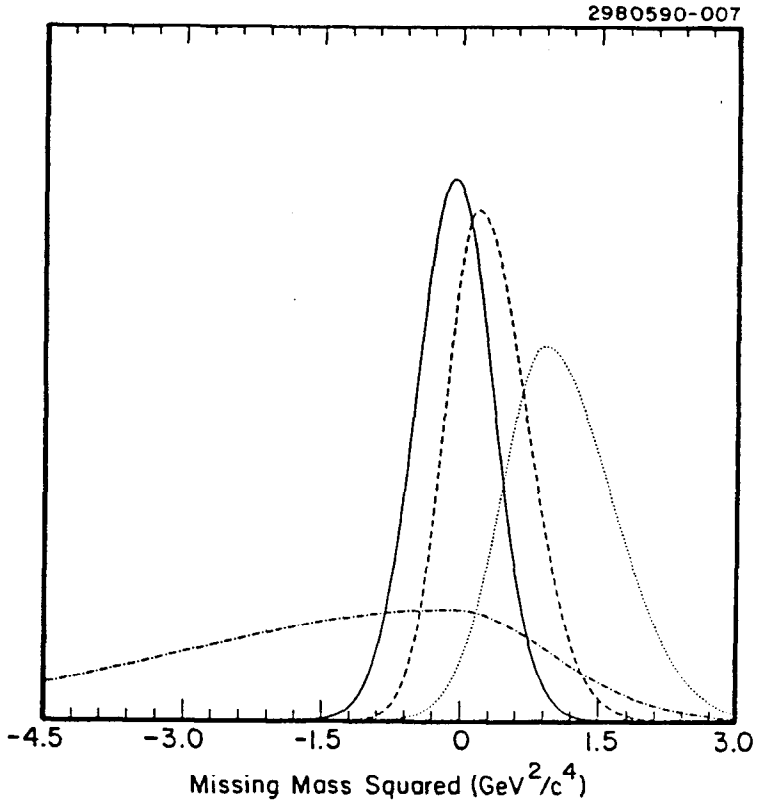

Figure 2. Missing mass squared distributions generated prediction by ISGW model (Ref. 6) and CLEO detector simulation. The decay modes shown are $\bar{B}\to Dl^-\bar{\nu}$ (solid line), $\bar{B}\to D^*l^-\bar{\nu}$, $D\to DX$ (dashed line), $\bar{B}\to D^{**}l^-\bar{\nu}$, $D^{**}\to DX$ (dotted line).

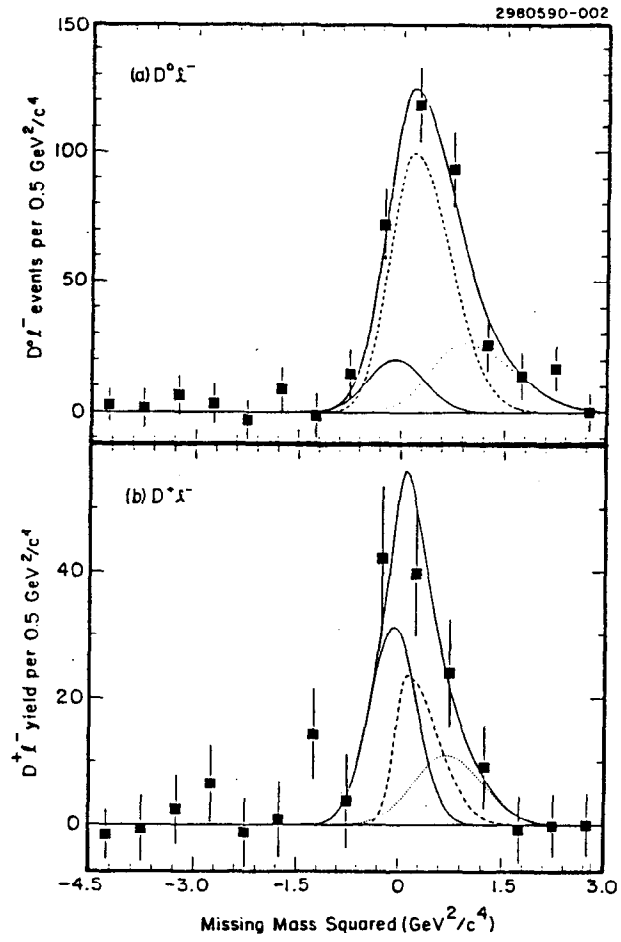

Figure 3. Missing mass squared (MM) distributions from fits to $K\pi(\pi)$ mass distributions. Data points show the D yields in the right sign combinations ($K^-\pi^+l^-$) in each MM bin, and the histogram shows the ones in wrong sign combinations ($K^-\pi^+l^+$).

contribution of process (d), we use the shape of the MM distribution from Monte Carlo simulation of mixed events, and the normalization determined from the number of Dl^+ combinations in order to improve the bin-to-bin statistical fluctuation of subtraction. The MM distributions after the subtraction are shown in Figure 4 for D^+l^- and D^0l^-.

In order to distiguish among processes (a-c), we utilize the differences in the D momentum spectra and MM distributions expected for them. The predictions by ISGW[6] are shown in Figure 5. The form factors are such that process (a) gives hard D spectrum (80% of D's have momenta above 1.5 GeV/c), whereas that from (b-c) is somewhat softer (only 50% of D's fall in the same momentum range). The predictions of other models[7,8] are very similar. The MM distribution from (a) centers almost exactly at zero with a width of about 0.3 $(GeV/c^2)^2$.[12] The MM distribution from (b) centers at 0.3 $(GeV/c^2)^2$ above (a), and that from (c) centers at 1 $(GeV/c^2)^2$ and extends above 2 $(GeV/c^2)^2$. In order to fully utilize these two variables, we make two MM distributions for D^+l^- (and two for D^0l^-): one with D momenta above 1.5 GeV/c; and the other below 1.5 GeV/c. We fit each MM distribution to the sum of the MM distributions predicted for the processes (a-c):

$$F(MM)=A_D F_D (MM)+A_{D^*}F_{D^*}(MM)+A_{D^{**}}F_{D^{**}}(MM),$$

where A_D, A_{D^*} and $A_{D^{**}}$ are the number of the D, D^* and D^{**}. The functions F_D, F_{D^*} and $F_{D^{**}}$ are normalized so that their integrals are unity. For each of the processes (a-c) we constrain the ratio of its contributions to high and low D momentum samples to the value ISGW[6] model predicts. Furthermore, the contribution of $\bar{B}^0 \to D^{*+} l^- \bar{\nu}$ is constrained using its measured branching fraction.[9] The results of the fits are shown in Figure 4 by a solid line along with the contribution from each process.

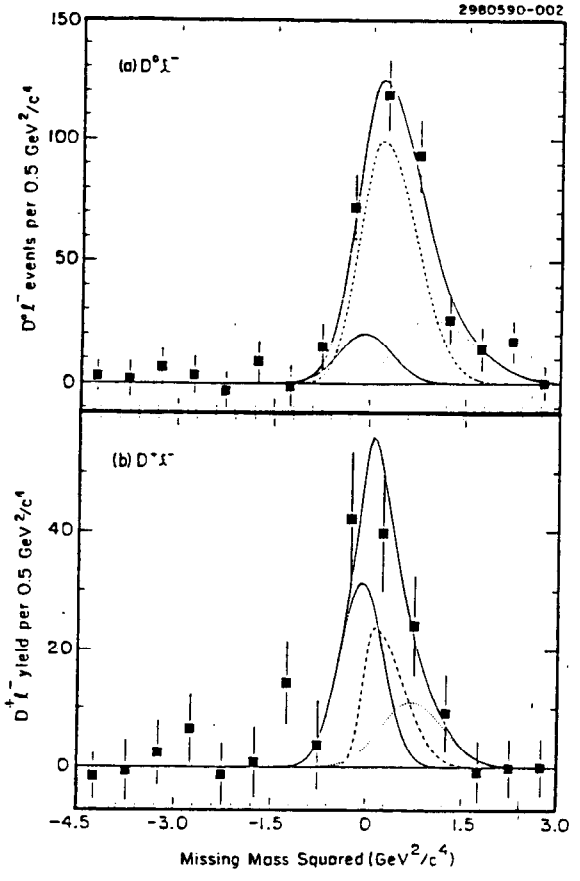

Figure 4. Missing mass squared distributions after subtracting the contribution from process where the D comes from one B and the lepton comes from the other B. The fits to the distributions in solid curve (higher one), as well as various components are displayed. $\bar{B} \to Dl^- \bar{\nu}$ (solid line), $\bar{B} \to D^* l^- \bar{\nu}$, $D \to DX$ (dashed line), $\bar{B} \to D^{**} l^- \bar{\nu}$, $D^{**} \to DX$ (dotted line).

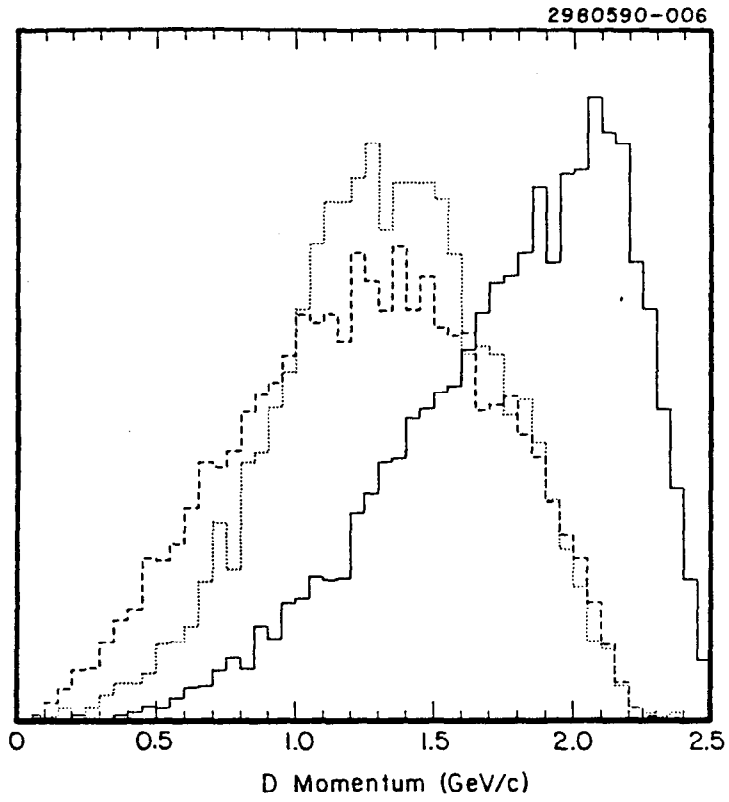

Figure 5. Momentum distribution of D's in semileptonic B decays, as predicted by ISGW model (Ref. 6) and CLEO detector simulation. The decay modes shown are $\bar{B}\to D l^- \bar{\nu}$ (solid line), $\bar{B}\to D^* l^- \bar{\nu}$, $D\to DX$ (dashed line), $\bar{B}\to D^{**} l^- \bar{\nu}$, $D^{**}\to DX$ (dotted line).

Since the sample with D^+ momenta below 1.5 GeV/c is dominated by already-measured $D^{*+} l^- \bar{\nu}$ decays[9] ($D^{*0} l^- \bar{\nu}$ decay does not feed into this mode) and, furthermore, the D^+ signal in that sample is statistically very weak due to a large combinatoric background, we do not use it.

Fitting the D^0 data alone yields the following number of D^0's for processes (a)-(c):

$$A_{D^0} = 42 \pm 14,\ A_{D^*}(D^0) = 218 \pm 35, \text{ and } A_{D^{**}}(D^0) = 79 \pm 29$$

in the entire D^0 momentum range, while fitting the D^+ data alone gives

$$A_{D^+} = 54 \pm 18, \text{ and } A_{D^{**}}(D^+) = 27 \pm 17$$

in the D^+ momentum range above 1.5 GeV/c. A_{D^*} is fixed using the $B(\bar{B}^0\to D^{*+} l^- \bar{\nu})$.[9]

If we impose in the fit an isospin symmetry constraint (the ratios of $D^* l^- \bar{\nu}$ and $D l^- \bar{\nu}$ rates are the same for the $\bar{B}^0$ and B^- decays):

$$\frac{\Gamma(\bar{B}^0\to D^{*+} l^- \bar{\nu})}{\Gamma(\bar{B}^0\to D^+ l^- \bar{\nu})} = \frac{\Gamma(B^-\to D^{*0} l^- \bar{\nu})}{\Gamma(B^-\to D^0 l^- \bar{\nu})},$$

we obtain

$A_{D^0} = 39 \pm 14$, $A_{D^*}(D^0) = 220 \pm 25$, and $A_{D^{**}}(D^0) = 79 \pm 28$; and
$A_{D^+} = 54 \pm 18$, and $A_{D^{**}}(D^+) = 27 \pm 16$.

Furthermore,

$$\frac{\Gamma(\bar{B}^0\to D^{*+} l^- \bar{\nu})}{\Gamma(\bar{B}^0\to D^+ l^- \bar{\nu})} = \frac{\Gamma(B^-\to D^{*0} l^- \bar{\nu})}{\Gamma(B^-\to D^0 l^- \bar{\nu})} = 2.6 \pm 1.1.$$

The fit gives a chi-squared per degree of freedom, χ^2/DF, of 0.5.

The branching fractions $B(\bar{B}^0 \to D^+ l^- \bar{\nu})$ and $B(B^- \to D^0 l^- \bar{\nu})$ can be calculated by

$$B(\bar{B}^0 \to D^+ l^- \bar{\nu}) = \frac{A_{D^+}}{2N_{4S} f_{+-} \varepsilon_{D^+} \varepsilon_l \varepsilon_S \varepsilon_X} \text{ , and}$$

$$B(B^- \to D^0 l^- \bar{\nu}) = \frac{A_{D^0}}{2N_{4S} f_{00} \varepsilon_{D^0} \varepsilon_l \varepsilon_S} ,$$

where $2N_{4S} = N_B = 480{,}000$ is the total number of B mesons, f_{+-} and f_{00} are the fractions of $\Upsilon(4S)$ decays to B^+B^- and $B^0\bar{B}^0$, ε_{Dl} is the efficiency for detecting the D in a semileptonic B decay, ε_l is the efficiency for finding a lepton with momentum $p_l > 1.4$ GeV/c (62% for electrons and 41% for muons,) ε_S is the lepton momentum acceptance, and ε_X is the fraction of the D^+ in the momentum range above 1.5 GeV/c. We obtain

$$B(\bar{B}^0 \to D^+ l^- \bar{\nu}) = (1.8 \pm 0.6 \pm 0.3)\frac{0.5}{f_{00}}\% \text{ , and}$$

$$B(B^- \to D^0 l^- \bar{\nu}) = (1.6 \pm 0.6 \pm 0.3)\frac{0.5}{f_{+-}}\% .$$

The former result agrees well with ARGUS result of $(1.6\pm0.5\pm0.5)(0.5/f_{00})\%$. The systematic errors are dominated by the uncertainties in the background estimate in the fit and the contribution of $\bar{B}^0 \to D^{*+} l^- \bar{\nu}$.

We obtain the branching fraction $B(B^- \to D^{*0} l^- \bar{\nu})$ from $A_{D^*}(D^0)$ after subtracting the contribution from $\bar{B}^0 \to D^{*+} l^- \bar{\nu}$ (87 events). We find

$$B(B^- \to D^{*0} l^- \bar{\nu}) = (4.1 \pm 0.8 \pm \frac{0.8}{0.9}\frac{0.5}{f_{+-}})\% .$$

Note that this result is not statistically independent from the previous two due to the isospin symmetry constraint we have introduced.

We calculate the rate for $\bar{B} \to D l^- \bar{\nu}$ using $\Gamma(\bar{B} \to D l^- \bar{\nu}) = B(\bar{B} \to D l^- \bar{\nu})/\tau(\bar{B})$. Since we do not know the lifetime of charged and neutral B mesons individually, we use the lifetime measured at higher energy e^+e^- colliders for an unknown mixture of various b-flavored particles, and assign 20% error to account for the uncertainty in this procedure. For $B(\bar{B} \to D l^- \bar{\nu})$ we use the average of $B(\bar{B}^0 \to D^+ l^- \bar{\nu})$ and $B(B^- \to D^0 l^- \bar{\nu})$ assuming $f_{+-} = f_{00} = 0.5$. The final result is only weakly dependent on the values of f_{+-} and f_{00} since when one branching fraction increases, the other decreases. We obtain

$$\Gamma(\bar{B} \to D l^- \bar{\nu}) = \frac{B(\bar{B} \to D l^- \bar{\nu})}{\tau(\bar{B})} = (1.5 \pm 0.4 \pm 0.4) \times 10^{10} s^{-1}.$$

This result implies that $|V_{bc}| = 0.037 \pm 0.005$ in the ISGW model and $|V_{bc}| = 0.043 \pm 0.006$ in the WSB[7] and KS[8] models. As our final result we average these two values (in the absence of a better way) and obtain $|V_{bc}| = 0.040 \pm 0.006 \pm 0.006$. The systematic error reflects the difference among the models. This agrees well with the result obtained from $B(\bar{B}^0 \to D^* l^- \bar{\nu})$ of (0.039 ± 0.004).

As noted above, we obtain the ratio of semileptonic widths for final states with vector and pseudo-scalar D mesons,

$$\frac{\Gamma(\bar{B}^0 \to D^{*+} l^- \bar{\nu})}{\Gamma(\bar{B}^0 \to D^+ l^- \bar{\nu})} = \frac{\Gamma(B^- \to D^{*0} l^- \bar{\nu})}{\Gamma(B^- \to D^0 l^- \bar{\nu})} = 2.6 \pm 1.1.$$

This is independent of the values of f_{00} and f_{+-} and is compatible with theoretical predictions, which vary from 2.3 to 3.1, as well as the value found by the ARGUS collaboration[13] of $3.3 \pm \frac{3.7}{1.1}$.

Isospin symmetry implies $\Gamma(\bar{B}^0 \to D^{*+} l^- \bar{\nu}) = \Gamma(B^- \to D^{*0} l^- \bar{\nu})$ and $\Gamma(\bar{B}^0 \to D^+ l^- \bar{\nu}) = \Gamma(B^- \to D^0 l^- \bar{\nu})$. Therefore, the lifetime ratio of charged and neutral B mesons can be calculated from the ratio of semileptonic branching fractions.

$$\frac{\tau(B^-)}{\tau(\bar{B}^0)} \frac{B(B^- \to D^{*0} l^- \bar{\nu})}{B(\bar{B}^0 \to D^{*+} l^- \bar{\nu})} = \frac{B(B^- \to D^0 l^- \bar{\nu})}{B(\bar{B}^0 \to D^+ l^- \bar{\nu})} = (0.89 \pm 0.19 \pm 0.13) \frac{f_{00}}{f_{+-}}.$$

The systematic error is dominated by the uncertainties in the determination of the background levels under the D peaks, and the size of $\bar{B}^0 \to D^{*+} l^- \bar{\nu}$ feeding into our Dl samples. This result is consistent with our previously published limits,[14] and a recent indirect measurement by ARGUS.[15] Theoretical predictions for this ratio lie in the range between 1.0 and 1.2. Note that this result is sensitive to the change in f_{00} and f_{+-}.

III. Observation of the Decay $D_S^+ \to \phi l^+ \nu$[16]

Although the D_S^+ meson has been observed in several decay modes, there have been no measurements of an absolute branching fraction. We accomplish this by observing the decay $D_S^+ \to \phi l^+ \nu$.

The branching fraction of the decay $D_S^+ \to \phi l^+ \nu$ can be calculated since the partial decay width may be inferred from the partial width for the decay $D^+ \to K^* l^+ \nu$. The difference in the form factors and decay phase spaces are such that

$$\Gamma(D_S^+ \to \phi l^+ \nu) = 0.8 \Gamma(D^+ \to K^* l^+ \nu).[17]$$

From the ratio of the lifetimes of these two particles,

$$\Gamma_{tot}(D_S^+) = 2.3 \Gamma_{tot}(D^+).[18]$$

Therefore, we obtain

$$B(D_S^+ \to \phi l^+ \nu) = 0.35 B(D^+ \to K^* l^+ \nu) = (1.55 \pm 0.37)\%.$$

Due to missing ν, the distribution of the invariant mass of ϕl^+ would not form a narrow Gaussian peak but rather extend from the threshold of 1 GeV/c^2 up to the D_S^+ mass of 1.97 GeV/c^2. Since the majority of the D_S^+ is produced in the momentum range above 2.5 GeV/c, and there are many fewer random background combinations in that momentum range than in the lower momentum range, we require that the momenta of ϕl^+ candidates be greater than 2 GeV/c, which approximately corresponds to the D_S^+ momentum of 2.5 GeV/c. We also require that the momentum of the ϕ be greater than 1 GeV/c. The implication of this cut is described later.

Figure 6 shows K^+K^- invariant mass distributions for events with either identified electrons or muons. As described above, the momentum and invariant mass requirements on the ϕl^+ candidates as well as the momentum requirement on the ϕ candidates have been imposed. There are 49 ϕ candidates in the electron sample and 26 in the muon sample.

Of those 75 ϕl^+ candidates, 16.6 are attributed to events with a ϕ and a hadron which is misidentified as a lepton. A sample of K_S^0 decays is used to estimate the probability that a π is misidentified as a lepton. In addition, in the $Y(4S)$ and $Y(5S)$ samples, which contain some $B\bar{B}$ events, we estimate based on the number of ϕ's and leptons per B decay that there are 4 random ϕ-l^+ combinations.

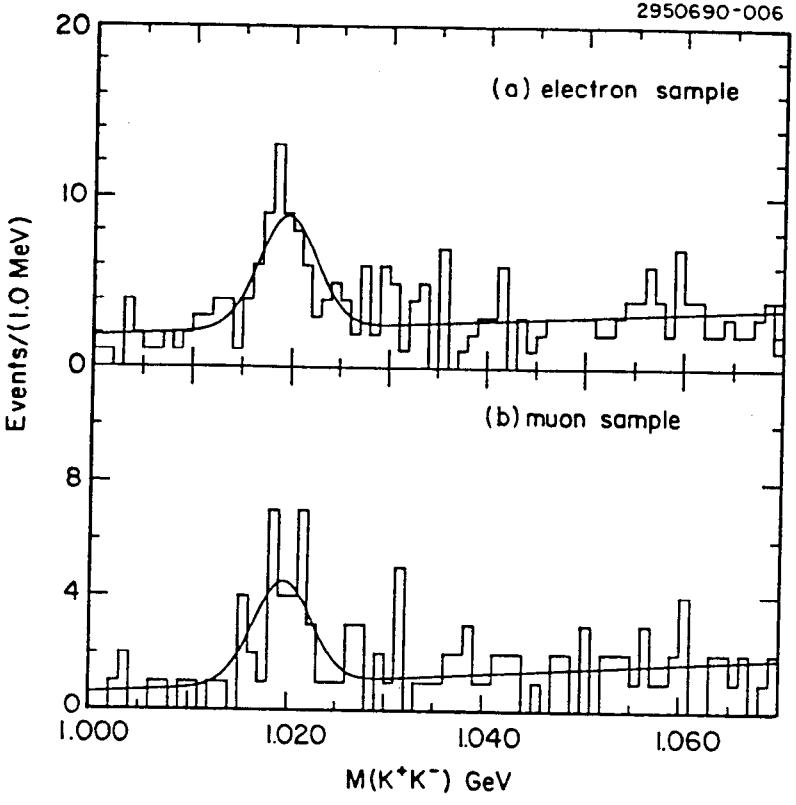

Figure 6. Invariant K^+K^- mass for events with identified leptons after kinematic cuts described in the text. The curves show the fits to the background and signal.

It is possible that a substantial number of our signal events are due to continuum random ϕ-l^+ combinations. Since the high momentum leptons which we use in this analysis come only from charmed particle decays, only if a ϕ is produced with charmed particles or from their decays, will a ϕ-l^+ combination result. Since neither the D^0 nor D^+ is likely to decay into ϕl^+ we ignore this contribution. The remaining source of background is:
(1) $e^+e^- \rightarrow c\,\bar{c}$ jets; c jet $\rightarrow D$ and ϕ; $D \rightarrow l^+X$, or
(2) $e^+e^- \rightarrow c\,\bar{c}$ jets; c jet $\rightarrow D$ and $\bar{c}$ jet $\rightarrow \phi$; $D \rightarrow l^+X$.

In order to investigate how often the ϕ is produced with charmed particles, we search for $D^{*+}l^+$ and D^0l^+ combinations using $D^{*+} \rightarrow D^0\pi^+$; $D^0 \rightarrow K^-\pi^+$ or $K^-\pi^-\pi^+\pi^+$ for D^{*+} and $D^0 \rightarrow K^-\pi^+$ for D^0. To study (1) and (2) separately, we consider two cases: one where the D and the ϕ are in the same hemisphere, and the other, in the opposite hemisphere, as shown in Figure 7. We reject events if the momenta of ϕ candidates are less than 1 GeV/c, since it is not easy to decide for these events whether the ϕ and the charmed meson come from the same jet or opposite jets in those events. There is an evidence for some ϕ's in the hemisphere opposite from the charmed mesons, but none is observed in the same hemisphere.

If a lepton and a ϕ come from the same jet, their invariant mass is very likely to fall below 2 GeV/c^2, whereas if they are from two different jets, their invariant mass will be higher than 2 GeV/c^2. From these observations, we conclude that there are at most 11 events in our signal from this source. Figure 8 displays ϕl^+ invariant mass distribution along with the sum of the estimate of various background contributions shown in solid histogram and signal, in dashed line.

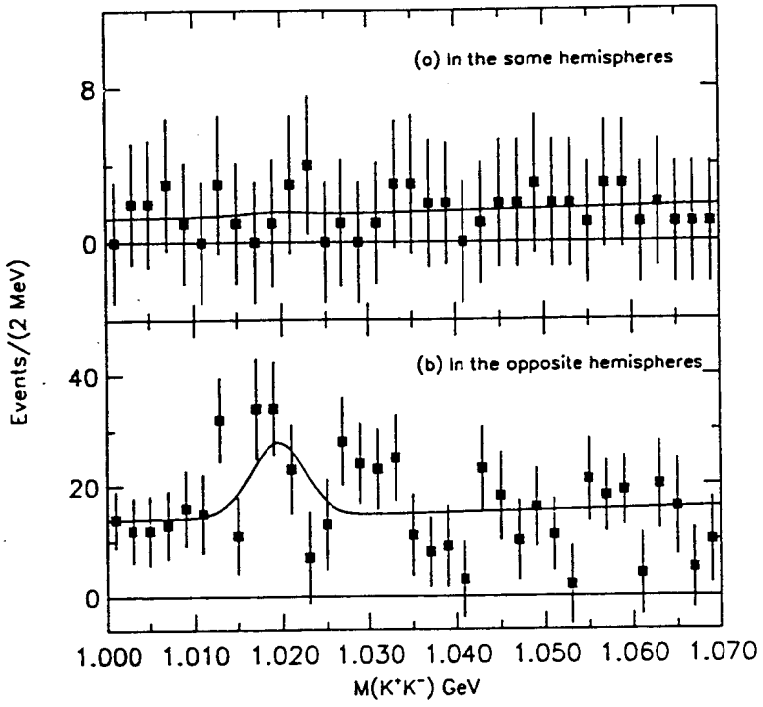

Figure 7. Invariant K^+K^- mass for events with identified D^0's or D^{*+}'s after kinematic cuts described in the text. The curves show the fits to the background and signal.

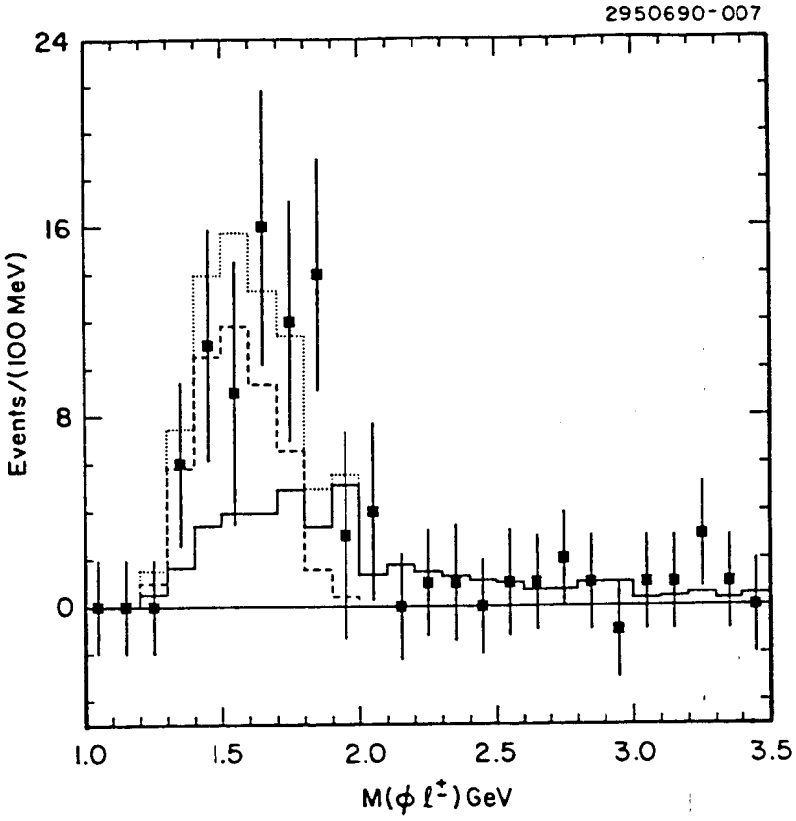

Figure 8. Invariant ϕl^+ mass distribution. The points are data. The solid histogram shows the sum of the expected background contributions. The dashed histogram shows the ϕl^+ mass for $D_S^+ \to \phi l^+ \nu$ decays using the model of ISGW (Ref. 6), normalized to the background subtracted data. The dotted histogram shows the sum of the solid and dashed histograms.

From the number of decays $D_S^+ \to \phi l^+ \nu$, we can obtain D_S^+ production cross section by

$$\sigma(D_S^+) = \frac{N_{D_S^+ \to \phi l^+ \nu}}{L\, B(D_S^+ \to \phi l^+ \nu)\, \varepsilon_{D_S^+ \to \phi l^+ \nu}},$$

where $N_{D_S^+ \to \phi l^+ \nu}$ is the number of $D_S^+ \to \phi l^+ \nu$ events observed, L is the total luminosity, and $\varepsilon_{D_S^+ \to \phi l^+ \nu}$ is the efficiency for detecting $D_S^+ \to \phi l^+ \nu$ decays. This gives rise to a D_S^+ production cross section of about a quarter nb^{-1} (or $R \sim 0.3$) at the center-of-mass energy of 10 GeV. Similarly, we obtain the absolute branching fraction for the decay $D_S^+ \to \phi \pi^+$ by

$$B(D_S^+ \to \phi \pi^+) = \frac{N_{D_S^+ \to \phi \pi}}{L\, \sigma(D_S^+)\, \varepsilon_{D_S^+ \to \phi \pi}} = \frac{N_{D_S^+ \to \phi \pi}\, \varepsilon_{D_S^+ \to \phi l^+ \nu}}{N_{D_S^+ \to \phi l^+ \nu}\, \varepsilon_{D_S^+ \to \phi \pi}} B(D_S^+ \to \phi l^+ \nu),$$

where $N_{(D_S^+ \to \phi \pi)}$ is the number of $D_S^+ \to \phi \pi$ events observed, and $\varepsilon_{D_S^+ \to \phi \pi}$ is the efficiency for detecting $D_S^+ \to \phi \pi$ decays.

We obtain

$$B(D_S^+ \to \phi \pi^+) = (3.1 \pm 0.6^{+0.9}_{-0.6} \pm 0.6)\%.$$

IV. $\Lambda_C^+ \to \Lambda \pi$ Decay Asymmetry[19]

Since the Λ_C^+ decays weakly, parity is not necessarily conserved in the decay. Bjorken[20] predicts that there should be a maximal parity violation in most of the Λ_C^+ decays, because the decay products in these decays are relativistic due to the Λ_C^+ mass, and therefore, the quark level expectation of $g_A/g_V \sim -1$ is preserved at the hadron level, giving $\alpha_{\Lambda_C^+} \sim -1$. In the decay $\Lambda_C^+ \to \Lambda \pi$, parity non-conservation might be observed as an asymmetric Λ distribution with respect to the Λ_C^+ spin direction, or an asymmetry in the Λ helicity. Since we do not *a priori* know the polarization of the Λ_C^+, we use the latter method to search for parity violation. If one observes only the helicity of the Λ, its polarization, $P_\Lambda = \alpha_{\Lambda_C^+}$. The angular distribution of the proton coming from the Λ decay is described by

$$\frac{dN}{d\cos\theta} = 0.5(1 + P_\Lambda \alpha_\Lambda \cos\theta) = 0.5(1 + \alpha_{\Lambda_C^+} \alpha_\Lambda \cos\theta), \qquad (1)$$

where θ is the angle between the directions of the Λ_C^+ and the π from the Λ decay in the Λ rest frame.

Figure 9 shows the distribution of $\Lambda\pi$ candidate invariant masses. The Λ candidates are required to decay 2 mm away from the production vertices. We also require that $x = p/p_{max} > 0.6$ and $|\cos\theta_h| < 0.8$, where p and p_{max} are the momentum of the $\Lambda\pi^+$ candidate and the kinematically allowed maximum momentum, and θ_h is the angle between the directions of the center-of-mass system and the Λ in the Λ_C^+ rest frame. We have combined charge conjugate modes (Λ_C^+ and $\bar{\Lambda}_C^-$). This is possible since although α's have opposite signs for a particle decay and its charge conjugate, the product of two α's for cascade decays has the same sign as their charge conjugate. There is clear evidence for the Λ_C^+. There is a second broader peak at the lower side of the first one. This may be due to the decay chain $\Lambda_C^+ \to \Sigma^0 \pi^+$ followed by $\Sigma^0 \to \Lambda\gamma$, where the γ is ignored. We repeat our analyses with and without this contribution and we include the difference as a systematic error, since we are not sure whether or not this second peak is real. In order to obtain the dependence of the rate on $\cos\theta$, we plot $\Lambda\pi$ invariant mass distributions for four $\cos\theta$ intervals.

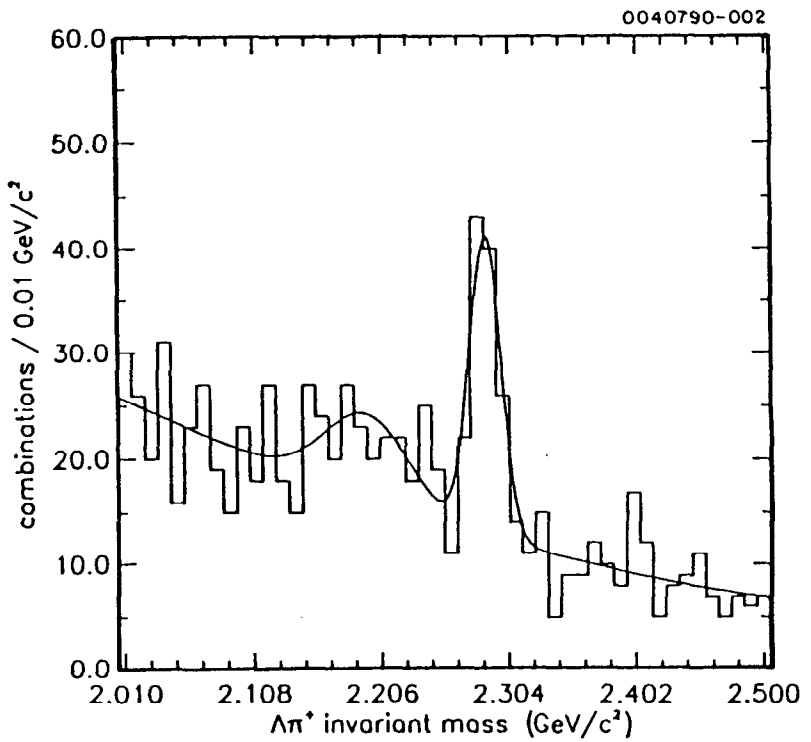

Figure 9. Invariant $\Lambda\pi^+$ mass distribution with $x=p/p_{max}>0.6$ and $|\cos\theta_h|<0.8$.

Figure 10 shows invariant mass distributions with the results of maximum likelihood fits described below. When $cos\theta$ is near -1, there is a strong Λ_c^+ signal, whereas there is almost no signal when $cos\theta$ is near +1. Figure 11 shows the production rates as a function of $cos\theta$, which are obtained by fitting the mass distributions with a Gaussian representing the Λ_c^+ signal and a polynomial background. Fitting the $cos\theta$ dependent rates to the equation (1) yields $\alpha_{\Lambda_c^+}=-1.1\pm0.4$. If we carry out the same analyses for the Λ_c^+ and $\bar{\Lambda}_c^-$ separately, we obtain $\alpha_{\Lambda_c^+}=-1.2\pm0.7$, and $\alpha_{\bar{\Lambda}_c^-}=+0.9\pm0.6$, which is consistent with $\alpha_{\Lambda_c^+} = -\alpha_{\bar{\Lambda}_c^-}$. This demonstrates the existence of parity violation in the decay $\Lambda_c^+\to\Lambda\pi$ at the 99% confidence level.

V. A Glance at CLEO II Data

The CLEO II detector, shown in Figure 12, started collecting data at the $\Upsilon(3S)$ resonance last summer. Its CsI crystal calorimeter has been working well and accomplished an energy resolution at 5.2 GeV of less than 1.5%. By observing the average energies calculated for Bhabha electrons as a function of time, we note that there are small systematic shifts in the energy, for which we have not found reasons. However, despite these shifts, the stability of the calorimeter is better than 0.2% (rms) over a period of a month. A preliminary study of photons arising from the decays $\Upsilon(3S)\to\gamma\chi_J$, where J=0, 1 and 2, we infer that the energy resolution near 100 MeV is about 4%. The energy distribution of the photons from the decay $B^*\to B\gamma$ (from data taken above B^* production threshold) indicates that the resolution in the 50 MeV range is about 8%, which is dominated by electronics noise.

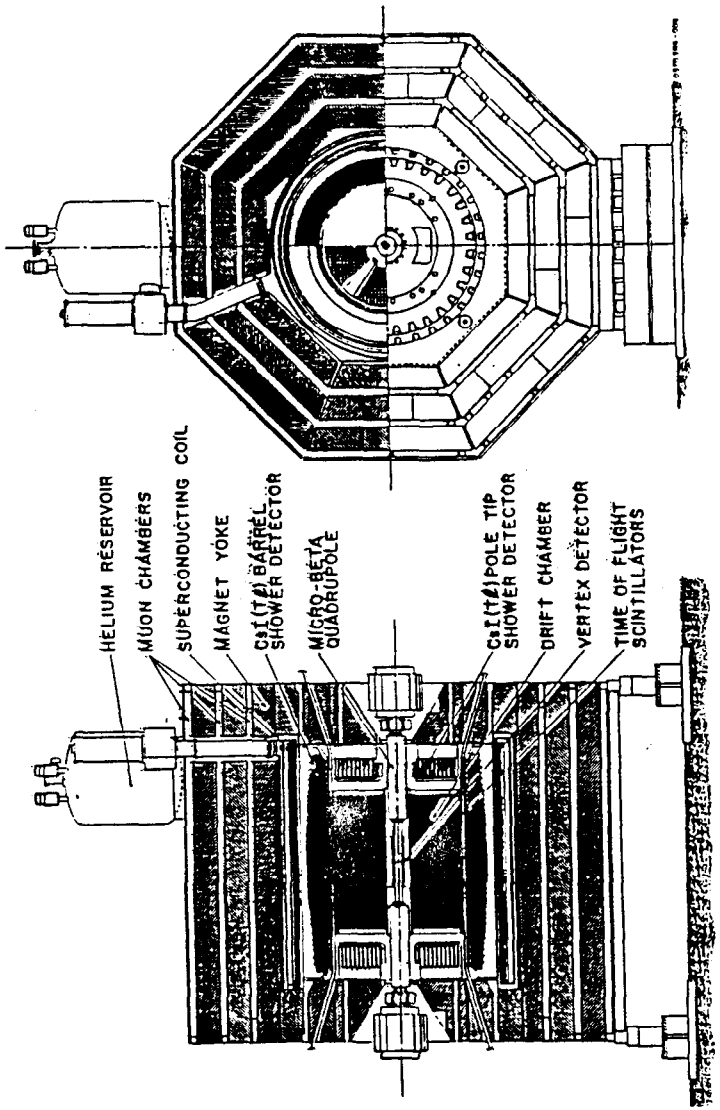

Figure 12. Schematic front and side views of the CLEO II detector.

Figure 13 shows a typical candidate for the sequential decays $\Upsilon(3S)\rightarrow\gamma\chi_J$; $\chi_J\rightarrow\gamma\Upsilon(1S)$; and $\Upsilon(1S)\rightarrow\mu^+\mu^-$. The calorimeter is free of noise.

In this paper we show only very preliminary results on one-prong τ decays using one-vs-one charged track topology events. Figure 14 shows $\gamma\gamma$ invariant mass distribution for one-vs-one events with only two photon candidates in one hemisphere, In Figure 15, the distribution of the invariant masses of $\pi^+\pi^o$ shows a prominent peak due to the ρ^+. We observe about 2,400 $\tau^+\rightarrow\rho^+\bar{\nu}_\tau$ in about 80 pb^{-1} of data. Notice that there are very few events beyond the τ mass, indicating that the background from $q\bar{q}$ annihilation events is very low.

Figure 16 shows a scatter plot of invariant masses of two pairs of γ's in one-vs-one topology events with 4 photon candidates in one hemisphere. Figure 17 shows the mass spectrum of the second $\gamma\gamma$ pair when the first pair is consistent with π^o, indicating that most of the background is due to matching wrong γ pairs. Again, $\pi^+\pi^o\pi^o$ invariant mass distribution, in Figure 18, suggests that the majority of these 670 events is due to a production of $a_1^+\rightarrow\pi^+\pi^o\pi^o$. There is only a handful of events with $\pi^+\pi^o\pi^o$ invariant masses greater than the τ mass, indicating again that the background from $q\bar{q}$ annihilation events is very low. This is in good contrast with CLEO I three-vs-one topology data resulting from $\tau^+\rightarrow\pi^+\pi^+\pi^-$ (instead of $\pi^+\pi^o\pi^o$). These data include about 17% of $q\bar{q}$ annihilation events since CLEO I was not capable of rejecting events with extra neutral energy clusters because the photon detection efficiency was low and there were too many spurious photon candidates.

In order to show one of CLEO II's potential capabilities for new physics, Figure 19 shows a scatter plot of invariant masses

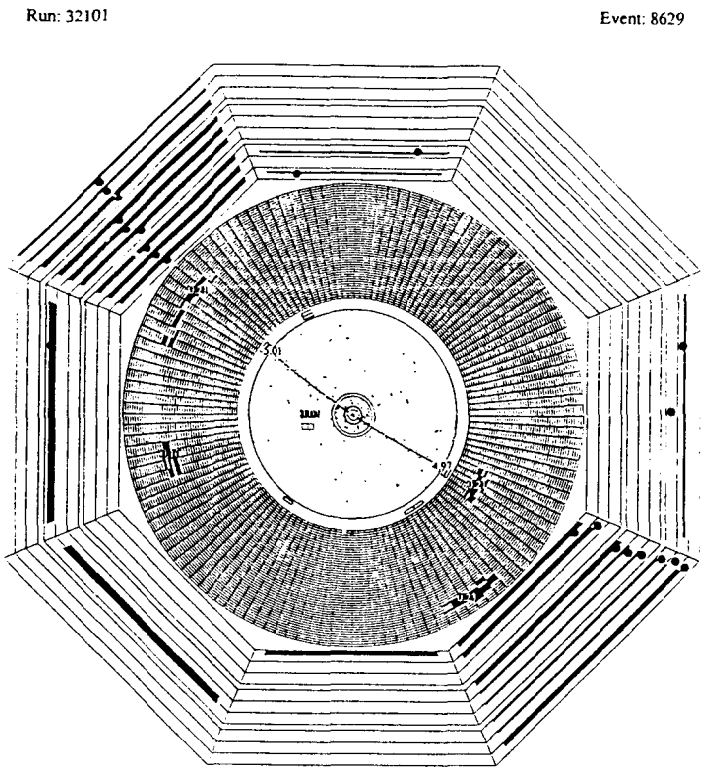

Figure 13. Candidate event for cascade decays $Y(3S)\rightarrow\gamma\chi_J$; $\chi_J\rightarrow\gamma Y(1S)$; and $Y(1S)\rightarrow\mu^+\mu^-$.

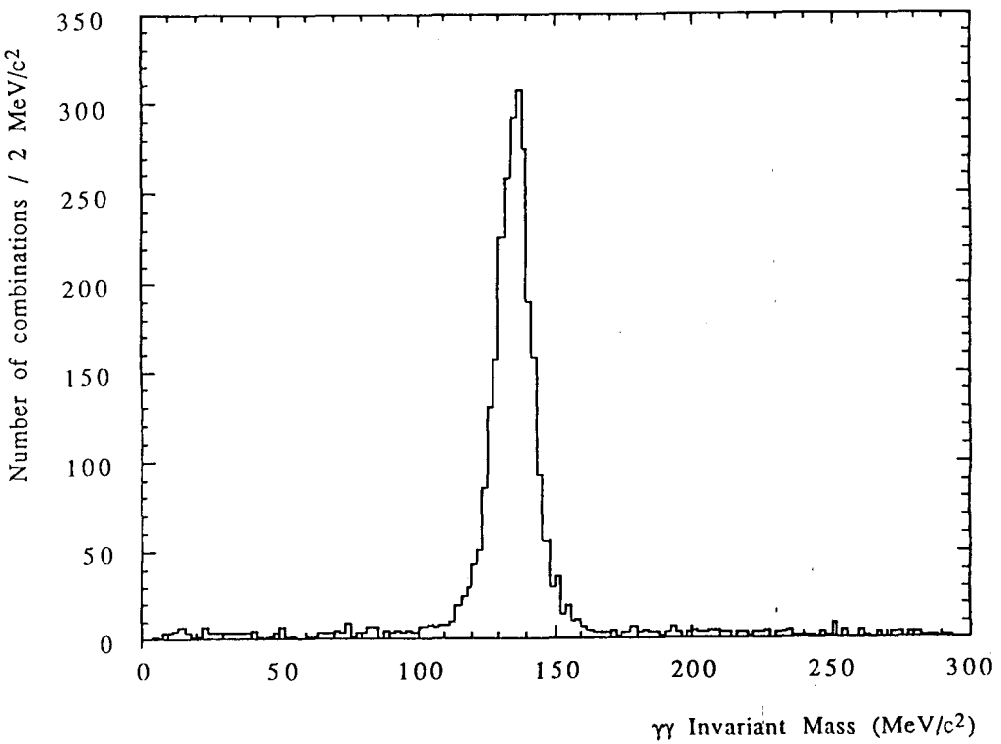

Figure 14. Invariant $\gamma\gamma$ mass distribution for one-vs-one topology two photon events.

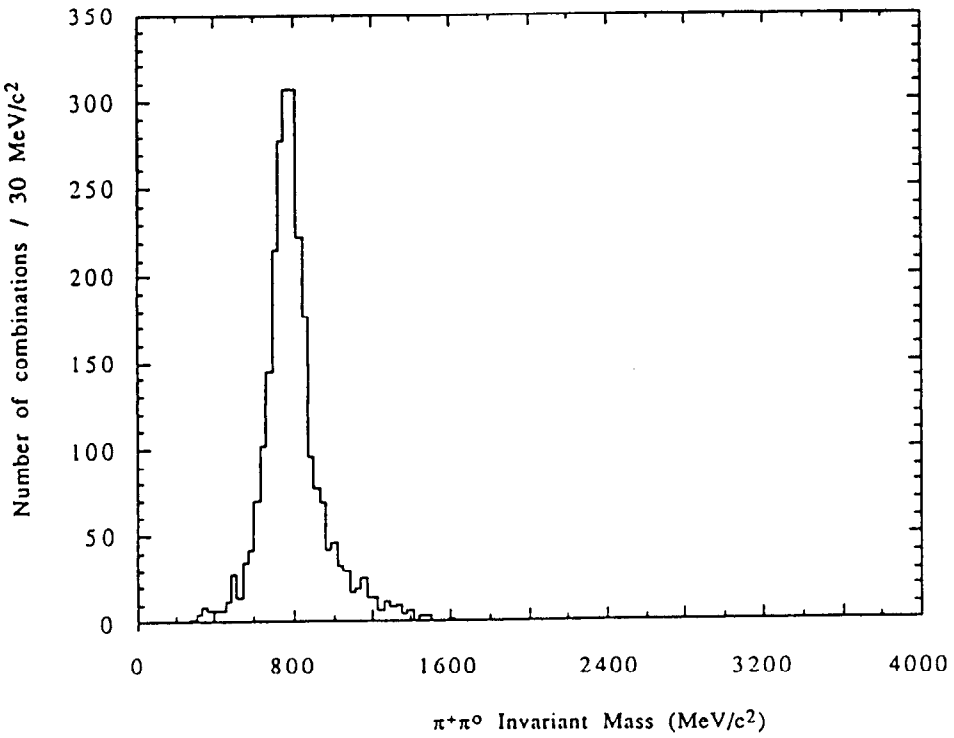

Figure 15. Invariant $\pi^+\pi^0$ mass distribution for the same events as Figure 14.

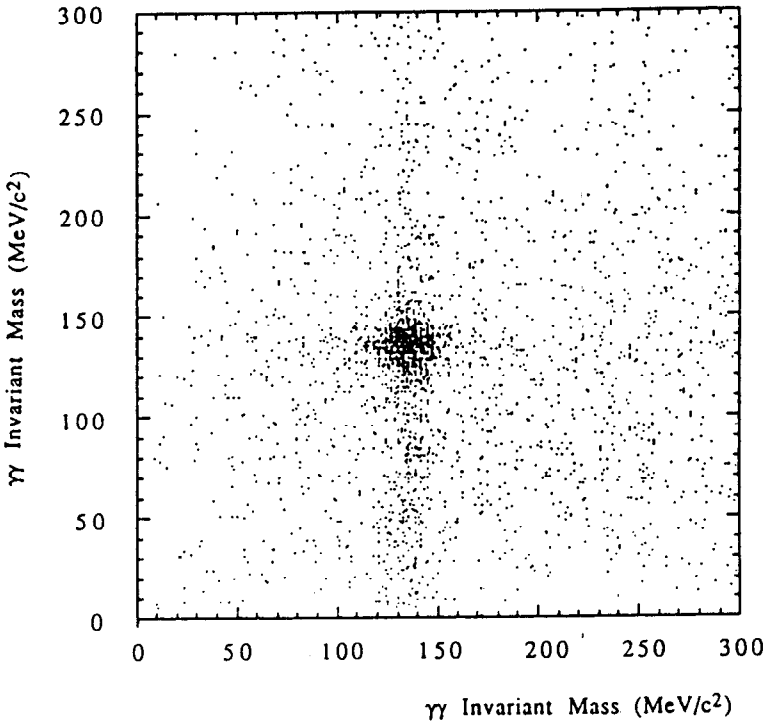

Figure 16. Scatter plot of invariant masses of two pairs of γ's in one-vs-one topology four photon events.

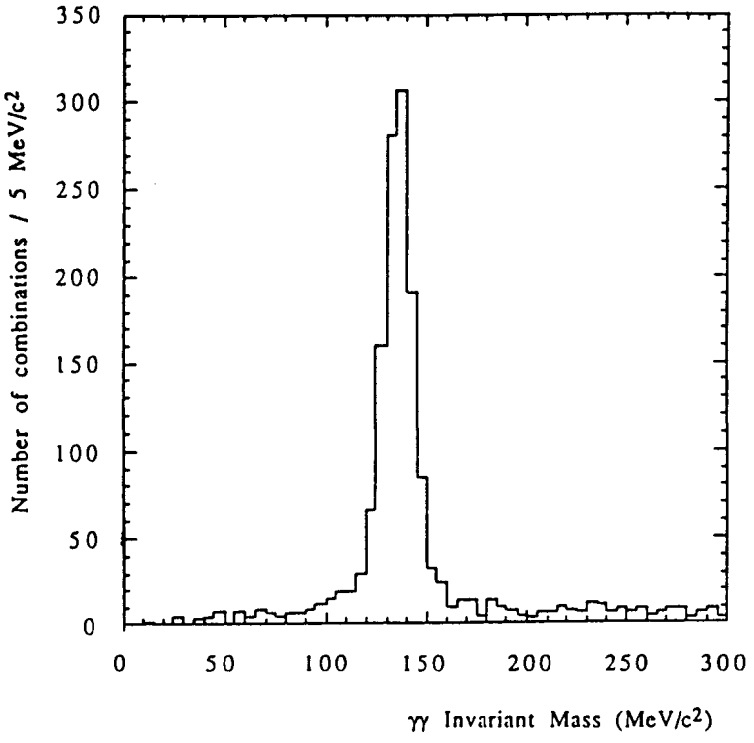

Figure 17. Invariant $\gamma\gamma$ mass distribution for one-vs-one topology four photon events when the other photon pair is consistent with π^0.

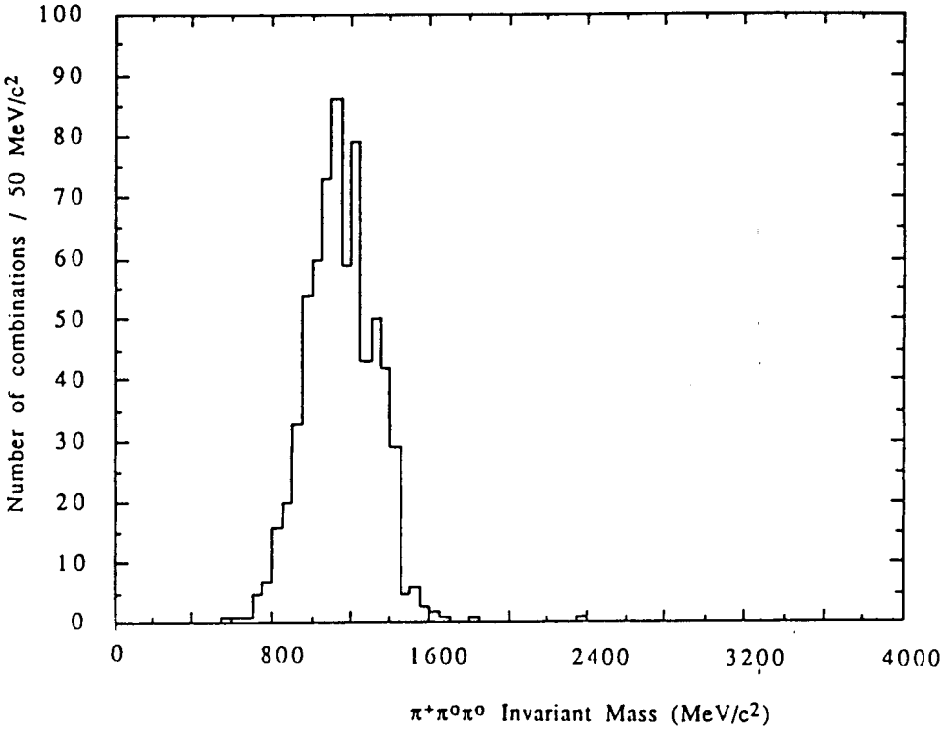

Figure 18. Invariant $\pi^+\pi^0\pi^0$ mass distribution for the same events as Figure 16.

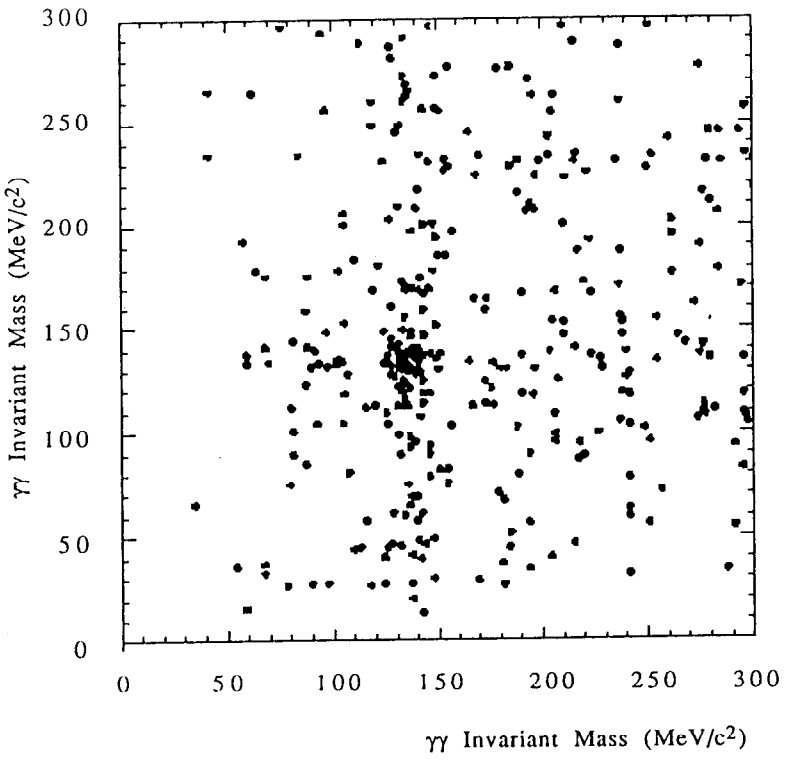

Figure 19. Scatter plot of invariant masses of two pairs of γ's in one-vs-one topology six photon events when third pair is consistent with π^0.

of two pairs of γ's in one-vs-one topology events with 6 photon candidates in one hemisphere. The third γ pair is required to form a π^0. There is a clear cluster of events which correspond to production of two additional π^0's in these events. (When the third γ pairs have masses outside the π^0 mass range, there is no enhancement correponding to two π^0 production in the scatter plot.) Most of the background is due to matching wrong γ pairs. Again, $\pi^+\pi^0\pi^0\pi^0$ invariant mass distribution, in Figure 20, suggests that the majority of these 68 events are due to τ decays, since there are no events with $\pi^+\pi^0\pi^0\pi^0$ invariant masses greater than the τ mass. In this case the major background to $\tau\to\pi^+\pi^0\pi^0\pi^0$ comes from other τ decays. We estimate that of those 68 events, 14 are random γ combinations (we have not taken out multiple counting of the same events.) An additional 18 can be attributed to $\tau^+\to\bar{\nu}_\tau\pi^+\pi^0$ and $\tau^-\to\nu_\tau\pi^-\pi^0\pi^0$. The remaining 36 events may be due to τ decays with more than one neutral particle, which would be the first direct evidence for such a decay mode.

VI. Conclusions

We have measured the branching fractions for $\bar{B}^0\to D^+l^-\bar{\nu}$ and $B^-\to D^0l^-\bar{\nu}$, and derived $|V_{bc}|=0.040\pm0.006\pm0.006$. The ratio of semileptonic widths for final states with vector and pseudo-scalar D mesons are determined to be 2.6 ± 1.1, and the ratio of B^- and $\bar{B}^0$ lifetimes, $\tau(B^-)/\tau(\bar{B}^0)=0.89\pm0.19\pm0.13$. We have observed the decay $D_S\to\phi l\nu$, and determined $B(D_S^+\to\phi\pi)=(3.1\pm0.6^{+0.9}_{-0.6}\pm0.6)\%$. The maximal asymmetry we have observed in the decay $\Lambda_c^+\to\Lambda\pi^+$ demonstrates a violation of parity conservation in the weak decay of a charmed particle.

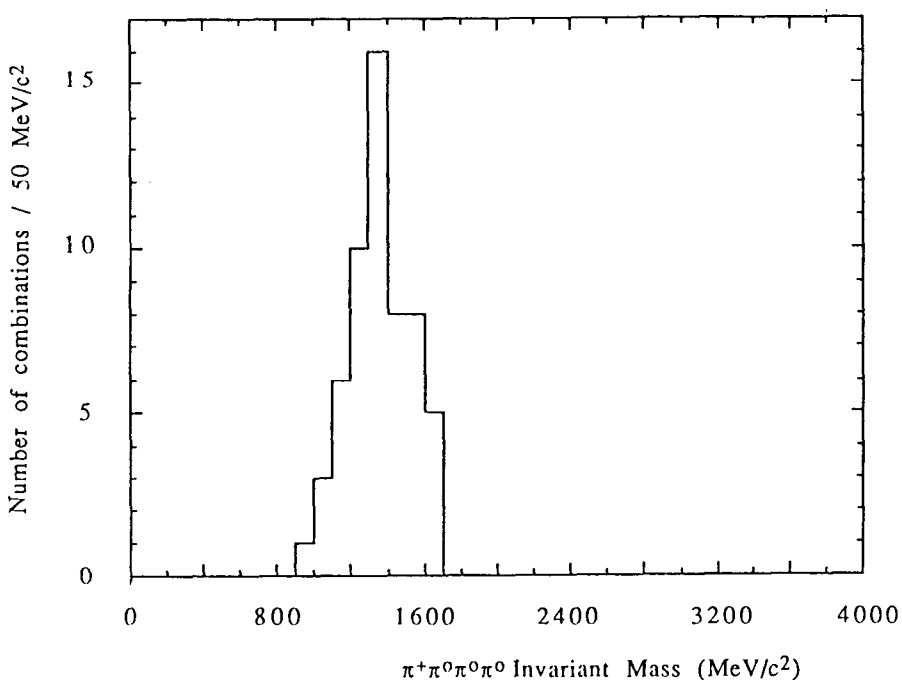

Figure 20. Invariant $\pi^+\pi^0\pi^0\pi^0$ mass distribution for the same events as Figure 18.

The CsI calorimeter of the CLEO II detector has shown that our expectation is reasonable, though we are still learning how to fully utilize it.

VII. Acknowledgements

I am grateful to the operating crew of the CESR storage ring. I am also indebted to everyone in the CLEO group. This work was supported in part by a grant from the Department of Energy under contract number DE-AC02-83ER40105 and in part by McKnight fellowship. Finally, I would like to thank the organizer of the SLAC Summer Institute for giving me an opportunity to participate in this wonderful experience.

References

1 CLEO Collaboration: D. Andrews *et al.*, Nucl. Instr. Methods **211**,47 (1983).

2 CLEO Collaboration: D.G. Cassel *et al.*, Nucl. Instr. Methods **A252**, 325 (1986).

3 CLEO Collaboration: T. Bowcock *et al.*, Phys. Rev. **D41**, 805 (1990).

4 "Exclusive and Inclusive Semileptonic Decays of B Mesons to D Mesons" The CLEO Collaboration, Cornell Preprint 90/989, July 1990. To be published in Phys. Rev. **D**.

5 S. Stone, "The Quark Mixing Matrix, Charm Decays and *B* Decays," in CP Violation, ed. by C. Jarlskog, World Scientific, Singapore, 1989, p.105.

6 B. Grinstein and M.B. Wise, Phys. Lett. **197B**, 249 (1987); N. Isgur, D. Scora, B. Grinstein and M.B. Wise, Phys. Rev. **D39**, 799 (1989).

7 M. Wirbel, B. Stech and M. Bauer, Z. Phys. **C29**, 269 (1985).

8 J.C. Körner and G.A. Schuler, Z. Phys. **C38**, 511 (1988).

9 CLEO Collaboration: D. Bortoletto *et al.*, Phys. Rev. Lett. **63**, 1667 (1989).

10 H. Albrecht *et al.*, Phys. Lett. **192B**, 245 (1987); M. Schäfer in the *Proceedings of the International Symposium on Heavy Quark Physics*, June 1989, Cornell University, Ithaca, NY, USA, AIP Conference Proceedings 196 (1989), eds. P.S. Drell and D.L. Rubin, p.97; M. Artuso *et al.*, Phys. Rev. Lett. **62**, 2233 (1989).

11 We include a minor correction in this calculation to account for contributions in process (d) from processes other than $B^0\overline{B}^0$ mixing.

12 The width is entirely due to our inability to know the B motion (p_B~0.3 GeV/c), which is assumed to be zero in the calculation of MM.

13 ARGUS Collaboration: H. Albrecht *et al*, DESY preprint 89-082.

14 CLEO Collaboration: A. Chen *et al.*, Phys. Rev. Lett. **52**, 1084 (1984).

15 ARGUS Collaboration: H. Albrecht *et al.*, Phys. Lett. **232B**, 554 (1989).

16 CLEO Collaboration: J. Alexander *et al.*, Phys. Rev. Lett. **65**, 1531 (1990).

17 N. Isgur *et al.*, Phys. Rev. **D39**, 799 (1989); M. Wirbel *et al.*, Z. Phys. **C29**, 269 (1985).

18 Particle Data Group, Phys. Lett. **237B**, 1 (1990).

19 "Measurement of the Λ_c^+ Decay-Asymmetry parameter" The CLEO Collaboration, Cornell Preprint CLNS 90/1013.

20 J. Bjorken, Phys. Rev. **D40**, 1513 (1989).